Vibron band structure in chlorinated benzene crystals: lattice dynamics calculations and Raman spectra of 1,4-dichlorobenzene

1989 J. Phys.: Condens. Matter 1 5051

(http://iopscience.iop.org/0953-8984/1/31/005)

J. Phys.: Condens. Matter 1 (1989) 5051–5064. Printed in the UK

Vibron band structure in chlorinated benzene crystals: lattice dynamics calculations and Raman spectra of 1,4-dichlorobenzene

A P J M Jongenelis†, T H M van den Berg‡, J Schmidt† and A van der Avoird‡

† Centre for the Study of Excited States of Molecules, Huygens Laboratory, Leiden University, PO Box 9504, Leiden, The Netherlands

‡ Institute of Theoretical Chemistry, University of Nijmegen, Toernooiveld, Nijmegen, The Netherlands

Received 6 February 1989

Abstract. Lattice dynamics calculations of the lattice modes (phonons) and the internal modes (vibrons) and Raman spectra at liquid helium temperatures are presented for the β-, α- and γ-phase of 1,4-dichlorobenzene (DCB). It follows from the calculations and it is confirmed by the Raman spectra that these three phases are characteristically different with respect to the following properties: vibron band dispersion, Davydov splitting, $^{35}Cl/^{37}Cl$ isotopic effects on the bandstructure and vibron–phonon mixing. Only the low temperature γ-phase shows a nice one-dimensional band structure for some vibrations. The vibron band dispersion in all phases of DCB is caused by the repulsive exponential terms in the intermolecular potential. This is in contrast to 1,2,4,5-tetrachlorobenzene, where the electrostatic interactions are responsible for the dispersion. Some of the *ungerade* vibron modes become visible in the Raman spectra of DCB due to the (random) occurrence of molecules with different distributions of $^{35}Cl/^{37}Cl$ isotopes. A few of the Raman lines observed could not be uniquely assigned; they are probably caused by Fermi resonances.

1. Introduction

Lattice dynamics calculations on 1,2,4,5-tetrachlorobenzene (TCB) have been described in a previous paper [1]. They were performed to obtain the dispersion and the splittings at $\boldsymbol{k} = 0$ of the coupled internal vibrations in the two phases of TCB. The intermolecular potentials used were based on the empirical atom–atom model [2–4]. It turned out to be essential to introduce polarised bonds, i.e. to add the electrostatic interaction to the atom–atom potential, in order to reproduce the experimentally observed [5] vibron band widths in α-TCB. The calculations showed that some of the vibrons are one-dimensional in the direction of the molecular stacks (the crystallographic $\boldsymbol{a}$ axis). The lattice modes and the lower vibron modes, however, did not show one-dimensional behaviour and the interactions between the stacks were also important for the overall crystal stability. It was further found that the splittings at $\boldsymbol{k} = 0$ in β-TCB are much smaller than in α-TCB. This finding was confirmed by Raman spectra. Moreover, the internal modes of the free TCB molecule were calculated for molecules with different $^{35}Cl/^{37}Cl$ isotopic mass distributions and the isotope shifts were compared with the calculated

0953-8984/89/315051 + 14 $02.50

vibron band widths. The calculated isotope splittings of the vibron bands were in very good agreement with the splittings observed in some of the Raman lines.

In this contribution, we present similar calculations of the dispersion of the coupled internal vibrations in the α-, β- and γ-phase of 1,4-dichlorobenzene (DCB). This crystal was chosen because it also exhibits a one-dimensional stacked crystal structure [6–11] and because investigations on the triplet electronic excitation by von Borczyskowski and co-workers [12, 13] show that the interaction between equivalent molecules in the stacks ($J_{\parallel}$) is about two orders of magnitude larger than the interaction between inequivalent molecules. Calculations of the lattice modes (phonons) of α- and β-DCB have been reported earlier, and in particular the frequencies at $\boldsymbol{k} = 0$ and the dispersion of the phonons have been investigated [2–4, 14, 15]. In addition, we calculate the effects of the different $^{35}Cl/^{37}Cl$ mass distributions on the vibron band structure. Raman experiments of the three phases at liquid helium temperatures are presented and confirm several aspects of the calculations.

2. Theory

The calculations are based on the standard harmonic lattice dynamics method, as extended to internal vibrations by Califano and co-workers [16, 17] and summarised in the previous paper [1]. We include the full self-term [18, 19] (equation (4) in reference [1]).

For the calculation of the vibrations of the free DCB molecule Scherer's generalised valence force field for chlorinated benzenes is used [20, 21]. Transformation from the stretch, bending, torsion and wagging coordinates to cartesian atomic displacements and solution of the **FG**-matrix problem in terms of the latter coordinates [22] yields six zero eigenvalues, which correspond with the three translations and the three rotations of the molecule, and 30 eigenvalues and eigenvectors which represent the normal modes of the free molecule.

The intermolecular potential is represented by an atom–atom potential of exp-6–1 type: $V(r_{ij}) = B\exp[-Cr_{ij}] - Ar_{ij}^{-6} + Dr_{ij}^{-1}$. Parameter sets for this potential, without the electrostatic parameter D, are given in [2, 4]. In order to obtain the correct vibron band widths for TCB, it was necessary to introduce polarised C–Cl and C–H bonds by including fractional atomic charges in both potential sets (charges of $-0.25e$ on Cl and $+0.25e$ on the corresponding C, and charges of $+0.10e$ on H and $-0.10e$ on the corresponding C) [1]. In this paper we have used four potential parameter sets: the parameters given in [2] or in [4], either with or without fractional atomic charges.

3. Molecular vibrations of DCB: isotopic effects

The vibrational normal modes of the free DCB molecule with D_{2h} symmetry were calculated and the resulting eigenvectors have been directly used in the lattice dynamics calculations. The calculated frequencies were replaced by the experimental values [20, 21] (as was also done for TCB [1]), although the calculated values are not very different.

The effect of chlorine isotopic substitution on the molecular frequencies is investigated by calculations on the three molecular species which can be formed with ^{35}Cl and ^{37}Cl atoms (natural abundance 3:1). We define the isotope shift of a specific vibration as

Table 1. Unit cell parameters for the three phases of DCB used in the lattice dynamics calculations and taken from [11]. The volume V of, and the number of molecules Z in the unit cell are also given.

	Unit cell parameters							
Phase	a (Å)	b (Å)	c (Å)	V (Å^3)	α (deg)	β (deg)	γ (deg)	Z
β at 300 K	7.361	5.963	3.959	159.4	92.13	113.24	91.42	1
α at 100 K	14.664	5.740	3.925	306.8	90	111.77	90	2
γ at 100 K	8.624	6.021	7.414	305.4	90	127.51	90	2

the (average) shift of the frequency of this vibration caused by the substitution of one ^{37}Cl atom by one ^{35}Cl atom. It is observed that the C–Cl stretch vibrations (328 cm^{-1} (A_g) and 550 cm^{-1} (B_{1u})) in particular are very sensitive to the chlorine mass, as is illustrated by their strong isotope shifts (4.0 cm^{-1} and 3.7 cm^{-1}). The (in-plane) C–Cl bend vibrations (226 cm^{-1} (B_{2u}) and 350 cm^{-1} (B_{3g})) show smaller shifts (1.6 cm^{-1} and 1.0 cm^{-1}). The out-of-plane vibrations show shifts that are very small, except for the 115 cm^{-1} (B_{3u}) vibration (0.8 cm^{-1}). The same behaviour was observed in the case of TCB where also the C–Cl stretch vibrations were most sensitive to the chlorine masses. In the lattice dynamics calculations the average chlorine mass of 35.453 amu is used. We return to the chlorine isotope effects after the presentation of the Raman spectra in § 5.

4. Lattice dynamics calculations on β-, α- and γ-DCB

4.1. Crystal structure and phonons

It is known that DCB can exist in three different phases. Under normal conditions DCB crystallises from the melt at 55 °C in the triclinic β-phase (space group $P\bar{1}$) with one molecule in the unit cell ($Z = 1$) [6], and transforms at 30.8 °C to the monoclinic α-phase ($P2_1/a$; $Z = 2$) [7, 8]. Below 0 °C a second monoclinic phase, the γ-phase, can exist with space group $P2_1/c$ and $Z = 2$ [9, 10]. In all phases the molecules are located at inversion centres and in α- and γ-DCB the orientations of the two molecules in the unit cell are related by reflection with respect to the *ac* plane. The positions and orientations of the molecules in the α- and β-phase were determined in the late 1950s [6–8] and the DCB molecules seemed to be heavily distorted in the crystal. More accurate and detailed x-ray studies of the three phases at different temperatures later became available [10, 11] and these new results showed that actually the DCB molecule in the crystal is almost regular and planar.

We have started the calculations by a structure optimisation of all three DCB phases, using planar DCB molecules with D_{2h} symmetry. The unit cell parameters for the three phases used in the calculations are given in table 1, and were fixed in the optimisation procedure. The optimised molecular orientations for all three phases calculated with the atom–atom potential sets given in [2] and in [4] are in good agreement with the results of the x-ray diffraction measurements [11]. The various potential sets give only small differences. Addition of fractional atomic charges hardly influences the optimised structure.

Table 2. The optical lattice mode frequencies of the three phases of DCB in cm^{-1}. The experimental values are from our Raman experiments performed at 1.2 K. The calculated values are obtained from a complete calculation including the vibrons using the potential set in [2] with the fractional atomic charges (see text). Values from the rigid body calculations are given in parentheses. The relatively large discrepancy between experiment and calculation for β-DCB is related to the fact that in the calculation the unit cell parameters for a crystal at room temperature are used. The frequencies calculated for β-DCB with the unit cell parameters at 100 K are 34, 50 and 102 cm^{-1}.

	Phonon frequencies (cm^{-1}) at $k = 0$					
	β-phase		α-phase		γ-phase	
Symmetry	Experiment	Calculation	Experiment	Calculation	Experiment	Calculation
(u)	—	— —	—	31 (31)	—	44 (44)
(u)	—	— —	—	37 (37)	—	49 (48)
(u)	—	— —	—	52 (52)	—	91 (88)
(g)	56	32 (32)	—	51 (51)	52	48 (48)
(g)	65	40 (40)	59	55 (55)	67	61 (59)
(g)	103	88 (89)	109	104 (107)	143	122 (127)
(g)	—	— —	33	30 (30)	76	62 (60)
(g)	—	— —	66	61 (61)	86	78 (82)
(g)	—	— —	117	110 (112)	133	115 (121)

In table 2 we present the optical phonon frequencies of the three DCB phases obtained in a complete calculation and in a rigid body calculation with the potential set given in [2] including fractional atomic charges. In addition we list the frequencies obtained in a Raman experiment at 1.2 K. Firstly, we discuss the phonon frequencies of β-DCB. From Raman experiments it is known that these frequencies are temperature dependent. Frequencies at 300 K of 46 cm^{-1}, 56 cm^{-1} and 90 $cm^{-1}$are reported [11], in agreement with 45 cm^{-1}, 56 cm^{-1} and 84 cm^{-1} from [3], and at 100 K frequencies of 54 cm^{-1}, 64 cm^{-1} and 99 cm^{-1} are reported in [11], compared with 56 cm^{-1}, 67 cm^{-1} and 102 cm^{-1} in [4]. In our calculation with the potential [2] with fractional charges we obtain lattice frequencies in reasonable agreement with the experimental frequencies reported at 300 K and with the calculated frequencies reported in [2, 3]. This agrees with the fact that we used the unit cell parameters obtained at this temperature. When the parameters of the 100 K crystal structure are used, all three calculated lattice frequencies increase in agreement with experiment [11]. From our calculations we see that the lattice frequencies, as in the case of TCB [1], are very sensitive to small deviations from the optimised crystal structure. Calculations with the other potential sets (see § 2) yield about the same results; the deviations are mainly caused by the small changes in the equilibrium orientation of the molecules. When the internal vibrations are included in the calculations the lattice frequencies change by less than 2 cm^{-1}, indicating a very small vibron–phonon mixing. The lattice modes show almost equal dispersion in all three directions of the Brillouin zone, leading to the conclusion that in this phase the interactions in all three crystallographic directions are important.

The lattice mode frequencies of α-DCB have been calculated using various potential sets. The results from different potentials differ by 5 cm^{-1} at most and the overall agreement with the experimentally observed and other calculated values [3] is good. In the complete calculation including the internal modes the lattice mode frequencies for

Table 3. Calculated splittings for $k = 0$ vibron frequencies and vibron band widths in all three directions of the Brillouin zone for α-DCB. The two columns in every direction refer to the width of the two bands. The potential set in [2] with charges is used. The potential set in [4] gives similar results. Calculations without fractional atomic charges hardly alter these numbers.

		α-DCB					
		Band width (cm^{-1})					
Vibration (cm^{-1})	Splitting (cm^{-1})	a^*		b^*		c^*	
115 (B_{3u})	6.8	−4.0	2.9	7.1	0.3	−15.0	−8.7
226 (B_{2u})	2.6	−1.3	1.3	8.6	6.0	5.3	3.8
298 (B_{2g})	0.9	−0.5	0.4	3.1	2.2	−2.9	−2.1
328 (A_g)	0.9	−0.4	0.4	−0.9	0.0	−0.8	0.0
350 (B_{3g})	0.7	−0.3	0.3	−1.3	−0.6	−0.8	−0.5
407 (A_u)	0.1	0.0	0.0	−4.6	−4.6	−0.2	−0.2
485 (B_{3u})	0.1	0.0	0.0	−0.5	−0.5	0.1	0.1
550 (B_{1u})	1.0	−0.5	0.5	−1.2	−0.2	−0.5	−0.1
626 (B_{3g})	0.1	0.0	0.0	1.6	1.6	0.6	0.6
687 (B_{2g})	0.0	0.0	0.0	0.5	0.5	0.5	0.5
747 (A_g)	0.6	−0.3	0.3	0.8	0.2	0.7	0.1
815 (B_{1g})	0.5	−0.5	0.0	−1.8	−1.3	−4.0	−2.2
819 (B_{3u})	3.5	−1.4	2.1	−1.1	1.4	−6.0	−4.1
934 (B_{2g})	0.2	−0.1	0.1	3.2	3.0	−1.1	−1.1
951 (A_u)	0.2	−0.1	0.1	−2.5	−2.5	−0.7	−0.7
1015 (B_{1u})	0.5	−0.2	0.2	0.5	0.0	0.8	0.5
1090 (B_{1u})	0.1	0.0	0.0	−1.6	−1.6	−1.3	−1.3
1096 (A_g)	0.4	−0.2	0.2	−0.4	0.1	−0.4	0.0
1107 (B_{2u})	0.2	−0.1	0.1	−3.2	−3.2	−2.4	−2.1
1169 (A_g)	1.4	−0.5	0.5	2.8	1.8	2.8	2.8
1221 (B_{2u})	0.5	−0.2	0.2	−0.2	0.2	0.7	0.2
1290 (B_{3g})	0.5	−0.2	0.2	3.4	2.9	2.8	2.6
1394 (B_{2u})	0.4	−0.2	0.2	−0.6	−0.1	−0.1	−0.1
1477 (B_{1u})	1.5	−0.7	0.7	−1.8	−0.3	−0.7	0.5
1574 (B_{3g})	0.0	0.0	0.0	0.1	0.1	0.4	0.4
1574 (A_g)	0.1	−0.1	0.0	−0.5	−0.4	−0.2	−0.1
3065 (B_{3g})	0.4	−0.2	0.2	1.0	0.6	1.4	1.0
3070 (A_g)	0.1	0.0	0.0	0.1	0.0	1.3	1.2
3090 (B_{2u})	0.4	−0.2	0.2	−0.8	−0.4	−0.2	0.2
3090 (B_{1u})	0.4	−0.1	0.0	−0.3	−0.2	−0.2	0.0

this phase also change by less than 2 cm^{-1}. The dispersion of the phonon frequencies calculated either with the potential set in [2] or with that in [4] is considerably smaller along $\boldsymbol{a}^*$ than along $\boldsymbol{b}^*$ and $\boldsymbol{c}^*$, indicating that the interactions in two crystallographic directions are more important than in the third ($\boldsymbol{a}$) direction. This is not surprising, since the distance between the molecules along the $\boldsymbol{a}$ axis is much larger than along the other two directions in the crystal. It will be seen that the calculated dispersion of the internal modes shows a similar behaviour.

The calculated lattice frequencies of γ-DCB show considerable differences (up to 14 cm^{-1}) when the potential parameters in [2] or [4] are used. We have checked that in this case the difference in optimised crystal structure does not account for the difference in phonon frequencies, but that it is really caused by the differences between the

potentials. Addition of charges hardly alters the frequencies. When performing a complete calculation the lowest phonon frequencies change by less than 2 cm^{-1}, but the highest lattice modes, with frequencies close to those of the lowest internal vibrations, change considerably (by up to 5 cm^{-1}). Also in the eigenvectors we observe (weak) mixing between the highest lattice modes and the lowest internal modes. In agreement with the experimental observations we see that the calculated lattice mode frequencies of γ-DCB are considerably higher than the frequencies of α-DCB. As in the α-phase the calculated dispersion is smallest in the $\boldsymbol{a}^*$ direction, in agreement with the fact that the distance between the molecules in the $\boldsymbol{a}$ direction in the largest. From these results it can be concluded that the dispersion, and thus the interaction, in both other directions is the most significant.

4.2. Davydov splittings of the vibrons

The internal modes in α- and γ-DCB are expected to be split into two components as a result of the presence of two symmetry related molecules in the unit cell (Davydov splitting). The splittings at $\boldsymbol{k} = 0$ calculated in α-DCB, given in table 3, are small ($\leqslant 1$ cm^{-1}) except for the 115 cm^{-1} (B_{3u}), 226 cm^{-1} (B_{2g}) and 819 cm^{-1} (B_{3g}) internal vibrations where we find splittings of up to 7 cm^{-1}. A small deviation from the optimised crystal structure has hardly any effect on the frequencies except for the lowest two internal vibrations. In the high frequency region the splittings are mainly caused by the fractional charges. Omitting these charges decreases the splittings at $\boldsymbol{k} = 0$: for the 819 cm^{-1} (B_{3u}) vibration from 3.5 cm^{-1} to a few tenths of a wavenumber. In the low frequency region either the r^{-6} term or the exponential term in the atom–atom potential gives the largest contribution to the Davydov splitting, but the effect caused by the dominant term is always partly compensated by an opposite contribution from the other part of the potential. The observation that either of these two terms of the potential can dominate the calculated Davydov splitting contrasts with the case of β-TCB, where the splitting in the low frequency region was mainly caused by the repulsive short-range interactions.

The calculated vibron frequencies at $\boldsymbol{k} = 0$ for γ-DCB, given in table 4, are similar to those in α-DCB, but since the phonon frequencies in γ-DCB are higher than in α-DCB mixing with internal vibrations is more significant. This explains the considerable splitting of 7.7 cm^{-1} for the 298 cm^{-1} (B_{2g}) vibration. Compared with α-DCB the overall splitting of the modes in γ-DCB is somewhat larger. The same decrease of the splittings as in α-DCB is observed in the 819 cm^{-1} region when the charges are omitted. Analysis of the origin of the splittings in the low frquency region shows that in γ-DCB the exponential terms of the potential give the largest contribution, which is partly compensated by an opposite effect from the r^{-6} term. This situation resembles that in β-TCB.

4.3. Vibron band structure

The computed vibron band widths for β-DCB are given in table 5 and clearly show that the dispersion in this system is not one-dimensional. Most vibrations have a band width which is smaller than 1 cm^{-1}, but some have a larger dispersion in one or in two directions. In contrast to TCB [1], addition of charges barely affects the widths of the vibron bands. The results hardly vary when using the potential sets [2] or [4] and, moreover, they are insensitive to small variations of the optimised crystal structure. The conclusion is that, just as for the lattice modes, the interactions responsible for the dispersion in β-DCB are of about the same size in all three crystallographic directions. We find that in all cases

Table 4. Calculated splittings for $k = 0$ vibron frequencies and vibron band widths in all three directions of the Brillouin zone for γ-DCB, using the potential set in [2] with charges. The potential set in [4] gives similar results. A calculation without charges hardly alters these numbers

		γ-DCB					
		Band width (cm^{-1})					
Vibration (cm^{-1})	Splitting (cm^{-1})	a^*		b^*		c^*	
115 (B_{3u})	7.4	−3.1	5.4	−6.6	0.8	−3.6	3.8
226 (B_{2u})	2.8	4.4	1.7	4.4	1.7	4.2	1.5
298 (B_{2g})	7.7	−0.9	0.5	7.2	−0.5	−3.4	4.3
328 (A_g)	0.6	0.0	0.0	0.6	0.0	0.5	0.0
350 (B_{3g})	0.0	−0.4	−0.4	−0.4	−0.4	−0.4	−0.4
407 (A_u)	0.2	0.3	0.3	−8.2	−8.0	0.2	0.0
485 (B_{3u})	2.1	0.0	0.0	−8.2	−6.1	−1.0	1.1
550 (B_{1u})	1.3	−0.7	0.0	−1.7	−0.4	−0.8	0.4
626 (B_{3g})	0.1	0.4	0.4	1.5	1.4	0.4	0.3
687 (B_{2g})	0.0	0.0	0.0	2.8	2.8	0.0	0.0
747 (A_g)	0.2	0.3	0.3	0.4	0.2	0.5	0.4
815 (B_{1g})	3.0	−1.7	−0.6	−3.3	−0.3	−2.7	0.3
819 (B_{3u})	3.6	4.0	1.8	6.0	2.4	−0.4	3.2
934 (B_{2g})	1.3	−0.4	−0.4	11.2	9.8	−1.1	0.2
951 (A_u)	0.2	0.4	0.4	−9.0	−8.8	−0.1	0.1
1015 (B_{1u})	0.4	−0.5	0.3	−0.2	0.2	−0.1	0.3
1090 (B_{1u})	0.3	−0.6	−0.6	−1.3	−1.1	−0.7	−0.6
1096 (A_g)	0.7	−0.2	0.2	0.7	0.0	−0.3	0.3
1107 (B_{2u})	1.5	−2.0	−1.9	−3.0	−1.5	−2.7	−1.2
1169 (A_g)	0.6	1.6	1.6	1.7	1.4	1.7	1.4
1221 (B_{2u})	0.1	0.0	0.0	0.1	0.0	0.0	0.0
1290 (B_{3g})	0.4	1.5	1.4	1.5	1.1	1.7	1.3
1394 (B_{2u})	0.1	−0.2	−0.2	−0.1	0.0	−0.1	0.0
1477 (B_{1u})	0.5	−2.3	−0.3	−0.9	−0.4	−0.9	−0.4
1574 (B_{3g})	0.0	0.2	0.2	0.0	0.0	0.2	0.2
1574 (A_g)	0.2	0.0	0.0	−0.3	−0.1	−0.1	0.1
3065 (B_{3g})	0.1	0.4	0.4	−0.8	−0.7	0.5	0.4
3070 (A_g)	0.3	0.8	0.5	−0.8	−0.5	0.8	0.5
3090 (B_{2u})	0.2	−1.1	−0.8	0.6	0.4	−1.0	−0.8
3090 (B_{1u})	0.3	−0.2	−0.1	0.8	0.5	−0.3	0.0

the repulsive exponential term gives the largest contribution to the dispersion, with some compensation from the attractive r^{-6} term. The large dispersion ($\simeq 10\ cm^{-1}$ along a^* and b^*) of the $328\ cm^{-1}$ (A_g) vibration is remarkable. As mentioned in § 3, this vibration is also very sensitive to the chlorine mass (isotope shifts of about $4\ cm^{-1}$). In § 5 we will discuss the Raman spectrum of this vibration in relation to the calculated results.

From the calculations on α-DCB (see table 3) we find that the dispersion of the internal vibrations is very small along a^* (except for the lowest vibrations) and large for some particular vibrations along b^* or along b^* and c^*. A calculation without the charges in the potential yields similar results. We have observed that the exponential terms in the atom–atom potential give the largest contribution to the band widths in the α-phase. The dispersion of some low frequency vibrations shows a considerable dependence on

Table 5. Calculated vibron band widths in all three directions of the Brillouin zone for β-DCB. The potential set in [2] with charges is used. The potential set in [4] gives similar results. Calculations without fractional atomic charges hardly alter these numbers.

	β-DCB		
	Band width (cm^{-1})		
Vibration (cm^{-1})	a^*	b^*	c^*
115 (B_{3u})	5.7	0.7	−5.4
226 (B_{2u})	3.9	3.7	3.7
298 (B_{2g})	−0.5	2.5	−1.0
328 (A_g)	10.0	10.3	−0.6
350 (B_{3g})	−0.5	−0.4	−0.4
407 (A_u)	−1.1	−6.2	−1.1
485 (B_{3u})	−1.1	−3.6	−2.1
550 (B_{1u})	−3.1	−4.0	0.0
626 (B_{3g})	0.2	1.0	0.5
687 (B_{2g})	0.4	1.8	0.6
747 (A_g)	1.0	1.0	0.6
815 (B_{1g})	1.7	0.2	−1.2
819 (B_{3u})	2.4	2.4	−5.5
934 (B_{2g})	1.0	5.2	0.3
951 (A_u)	−1.2	−4.8	−1.9
1015 (B_{1u})	−0.3	0.2	0.6
1090 (B_{1u})	−0.6	−1.2	−1.5
1096 (A_g)	0.0	0.2	0.2
1107 (B_{2u})	−1.8	−2.5	−2.3
1169 (A_g)	1.4	1.7	2.7
1221 (B_{2u})	−0.2	−0.2	0.4
1290 (B_{3g})	1.1	1.6	2.8
1394 (B_{2u})	−0.3	−0.1	−0.1
1477 (B_{1u})	−1.2	−0.7	−0.2
1574 (B_{3g})	0.1	0.1	0.3
1574 (A_g)	0.0	−0.3	−0.1
3065 (B_{3g})	0.0	0.0	1.0
3070 (A_g)	−0.1	−0.2	1.0
3090 (B_{2u})	−0.6	0.1	0.0
3090 (B_{1u})	0.4	−0.3	−0.8

the molecular orientations. This effect may be caused by the weak mixing with the lattice modes, which we have found to be sensitive to changes of the crystal structure. We therefore conclude that α-DCB, which was believed to represent a nice one-dimensional crystal [12, 23, 24] with respect to the delocalisation of the internal vibrations, is not one-dimensional at all.

When examining the band widths for γ-DCB, which are given in table 4, a striking difference with the two other phases is observed. Like in α- and β-DCB (and like in the one-dimensional system TCB [1]) the lowest vibrations exhibit dispersion in all three directions. Some higher modes, however, such as 407 cm^{-1} (A_u), 485 cm^{-1} (B_{3u}), 687 cm^{-1} (B_{2g}), 934 cm^{-1} (B_{2g}) and 951 cm^{-1} (A_u), show a clear one-dimensional dispersion up to 11 cm^{-1} along b^*. As in the other two phases, the main contribution originates from the exponential term in the potential and the charges hardly alter the results. Since there are no experimental data on the dispersion of the vibrations in γ-DCB it is impossible

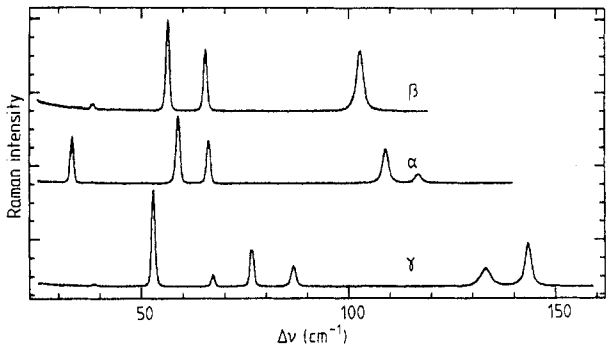

Figure 1. Raman spectra of the lattice modes of β-, α- and γ-DCB taken at a temperature of 1.2 K with a resolution of 0.8 cm^{-1}. The energy scale gives the difference in cm^{-1} from the 4880 Å laser line which was used for excitation.

as yet to verify these results. Our calculations suggest that the low-temperature phase is an attractive candidate for a quasi one-dimensional model system.

5. Raman experiments

5.1. Experimental procedure

In the Raman experiments we have studied β-, α- and γ-DCB at liquid helium temperatures. The experimental arrangement used in the Raman experiments has been described in detail in our previous paper [1]. DCB single crystals were obtained in the following way. 1,4-dichlorobenzene purchased from BDH (British Drug Houses Ltd.) was zone-refined for 100 passes.The resulting product was analysed by gas chromatography and contained less than 500 ppm of DCB isomers or other impurities. Neat crystals of β-DCB were grown from the melt by the Bridgman technique and subsequently annealed to reduce structural imperfections. To maintain DCB in the β-phase the crystal was cooled down quickly to liquid nitrogen temperatures. To obtain α-DCB a β-phase crystal was cooled very slowly, especially around the phase transition at 30.8 °C. These crystals were then stored at 10 °C where the α-phase is known to be most stable. By quick cooling of this sample it was possible to maintain the α-phase at liquid helium temperatures. As discussed in [9], the γ-phase is created by storing an undercooled β-phase crystal for some time at −10 °C.

5.2. Results and discussion

In figure 1 we present the Raman spectra of the lattice modes of all three phases of DCB obtained at 1.2 K. Since the linewidths at this temperature are small (about 0.8 cm^{-1}) the peaks in these spectra are well resolved, in contrast to previously reported spectra which were taken at about 100 K[9]. The frequencies of the lattice modes are all in good agreement with previously reported values and are given in table 2.

It is interesting to investigate whether the effects observed in the Raman spectra of TCB (isotope effects, site splitting and the observation of *ungerade* vibrations) can also be detected in the Raman spectra of DCB. Since both α- and γ-DCB have two molecules in the unit cell which are related by crystal symmetry, we cannot observe site splittings in these spectra. However, it should be possible to observe a Davydov splitting of the lines.

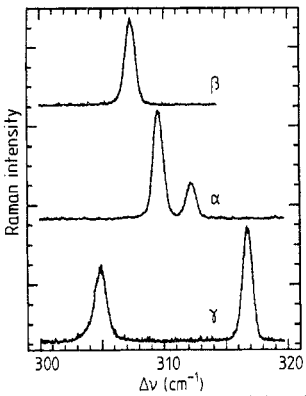

Figure 2. Raman spectra of the 298 cm^{-1} (B_{2g}) C–Cl out-of-plane vibration of β-, α- and γ-DCB. Conditions are as detailed in figure 1.

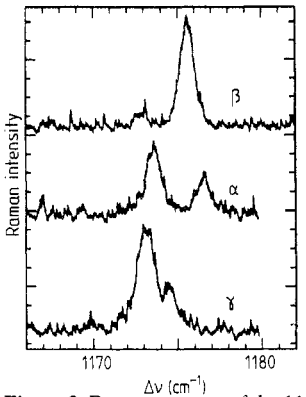

Figure 3. Raman spectra of the 1169 cm^{-1} (A_g) in-plane C–H bend vibration of β-, α- and γ-DCB. Conditions are as detailed in figure 1.

A beautiful example of such a Davydov splitting is presented in figure 2, where we show the Raman spectra of the 298 cm^{-1} (B_{2g}) vibration. The β-phase spectrum shows a single line, consistent with the fact that β-DCB has only one molecule in the unit cell. However, both α- and γ-DCB show a doublet. From the calculations summarised in § 3 we conclude that a splitting of this mode as a result of the different chlorine isotopes should be small and probably not detectable with our resolution. Bellows and co-workers [25] concluded, on the basis of the merging of the two lines in an isotopically mixed α-DCB crystal, that this splitting is a Davydov splitting. Comparison of our experimentally observed splittings with the calculated ones (see tables 3 and 4) shows good qualitative agreement. For α-DCB we measure a splitting of 2.6 cm^{-1} and calculate 0.9 cm^{-1} and for γ-DCB we measure about 12 cm^{-1} and calculate 7.7 cm^{-1}. So, even though γ-DCB seems a more one-dimensional system than α-DCB (if we consider the higher frequency internal vibrations), the Davydov splitting for this low frequency vibration in the γ-phase is considerably larger owing to its mixing with the higher frequency lattice modes.

The vibronic line in the $T_0 \rightarrow S_0$ phosphorescence spectrum of α-DCB, related to this 298 cm^{-1} C–Cl out-of-plane vibration also shows a double peak spectrum, which was previously attributed to a transition from the one-dimensional triplet exciton to a one-dimensional vibrational exciton [23]. With this assumption, a triplet exciton band width of about 1 cm^{-1} was obtained from phosphorescence spectra at various temperatures. Since in the 298 cm^{-1} vibron mode the Raman spectrum exhibits a Davydov splitting of 2.6 cm^{-1} and more accurate measurements show no variation of the phosphorescence lineshape with the temperature, it is clear that the structure in the phosphorescence spectrum is due to a Davydov splitting and that this observation cannot be used for determination of the triplet exciton band width.

Another Davydov splitting, shown in figure 3, is observed for the 1169 cm^{-1} (A_g) vibration. In the β-phase spectrum a single line is observed at 1176 cm^{-1} which is attributed to this vibration. In both α- and γ-DCB this line is split by about 3.5 cm^{-1} and 2 cm^{-1}, respectively, probably due to a Davydov splitting. The calculations predict a splitting of about 1.4 cm^{-1} for the α-phase and a splitting of about 0.6 cm^{-1} for the γ-phase. When a potential set without the Coulomb term is used, the calculated Davydov splittings in both phases are smaller than 0.1 cm^{-1}.

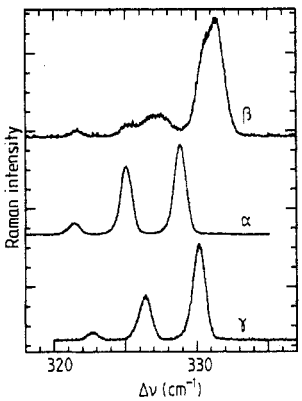

Figure 4. Raman spectra of the 328 cm^{-1}(A_g) C–Cl stretch vibration of β-, α- and γ-DCB. Conditions are as detailed in figure 1.

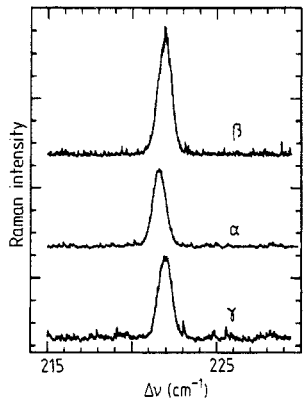

Figure 5. Raman spectra of the 220 cm^{-1} region of β-, α- and γ-DCB. The signal is attributed to the 226 cm^{-1} (B_{2u}) C–Cl bend vibration. Conditions are as detailed in figure 1.

In figure 4 we present the Raman line corresponding to the 328 cm^{-1} (A_g) vibration. Both for the α- and for the γ-phase we observe three lines separated by about 4 cm^{-1}, with an intensity ratio of about 1:6:9 and linewidths of $\simeq$1.0 cm^{-1}. From this ratio Bellows and co-workers [25], who studied α-DCB, concluded that all three lines belong to the 328 cm^{-1} (A_g) vibration and that they are caused by the different isotopic DCB species. This is confirmed by our calculation of the free molecule frequencies, where it is seen that this vibration is very sensitive to the chlorine mass and that the three peaks should indeed be separated by 4 cm^{-1} (see § 3). The fact that the three different isotopic species can actually be observed separately in the Raman spectra agrees with the lattice dynamics calculations on α- and γ-DCB from which we see that the dispersion of this vibration ($\leq$1 cm^{-1}) is much smaller than the frequency shift caused by the isotopes. As discussed in [1] this corresponds to a situation where a vibrational excitation is localised on clusters of molecules of the same isotopic species (the separated band limit). In β-DCB the situation is different. We calculate a band width of about 10 cm^{-1} for this vibration. The intermolecular coupling is therefore comparable with the intramolecular isotopic shift, which implies that the different isotopic DCB species are more or less amalgamated in the vibron band. We expect to observe one line in the Raman spectrum which may have a complicated structure. As can be seen in figure 4 the β-phase spectrum differs considerably from the other two spectra and the peak structure is very complex indeed. Since the calculations show that the isotope effects are small for all *gerade* vibrations, except the for 328 cm^{-1} (A_g) vibration, it is not surprising that in the Raman spectra of the other vibrations no effects of the different chlorine masses can be detected.

The breaking of the selection rules due to isotopic disorder, which caused some of the *ungerade* modes in TCB to become visible in the Raman spectrum (see [1]), is also observed in DCB. The *ungerade* vibrations in the Raman spectrum will be most intense for the DCB molecules with the lowest symmetry: molecules with one ^{35}Cl and one ^{37}Cl. This means that instead of the three lines originating from all isotopic species we observe only a single line. In figure 5 it can be seen that in the spectra of all three DCB phases we indeed observe a single line at about 222 cm^{-1}, which we attribute to the 226 cm^{-1} (B_{2u}) vibration. The same effect is illustrated in figure 6 where in the region around 530 cm^{-1} a single line is also observed, which we attribute to the 550 cm^{-1} (B_{1u}) vibration. These two *ungerade* vibrations are indeed most sensitive to the chlorine mass (see § 3).

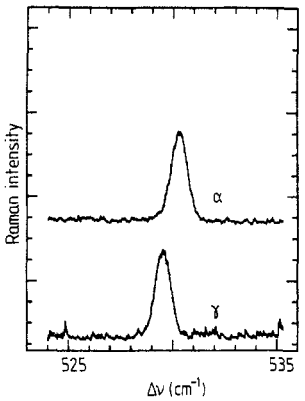

Figure 6. Raman spectra of the 530 cm^{-1} region of α- and γ-DCB. The signal is attributed to the 550 cm^{-1} (B_{1u}) C–Cl stretch vibration. Conditions are as detailed in figure 1.

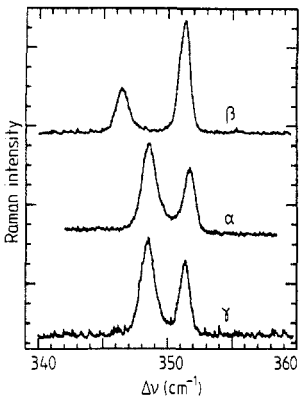

Figure 7. Raman spectra of the 350 cm^{-1} (B_{3g}) in-plane C–Cl bend vibration of β-, α- and γ-DCB. Conditions are as detailed in figure 1.

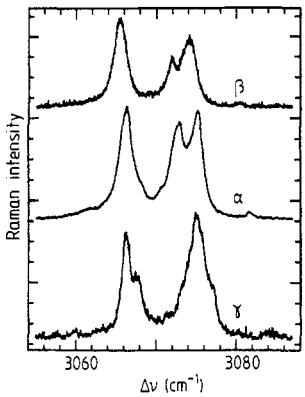

Figure 8. Raman spectra of the 3065 cm^{-1} (B_{3g}) C–H stretch and the 3070 cm^{-1} (A_g) C–H stretch vibration of β-, α- and γ-DCB. Conditions are as detailed in figure 1.

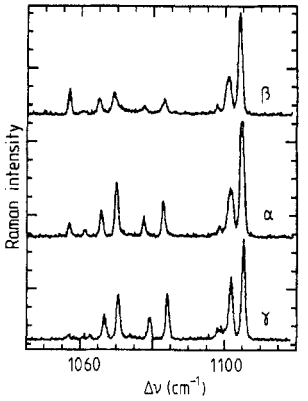

Figure 9. Raman spectra from 1050 cm^{-1} to 1110 cm^{-1} of β-, α- and γ-DCB. Conditions are as detailed in figure 1.

Besides the observations mentioned above, some intriguing phenomena are observed in the Raman spectra. For instance, in figure 7 we show the spectra of the 350 cm^{-1} region. A splitting in the Raman spectrum of α-DCB in this region was observed [25] and it was concluded, using the same arguments as for the 298 cm^{-1} vibration, that this splitting is a Davydov splitting. However, β-DCB contains only one molecule in the unit cell which eliminates the possibility of a Davydov splitting in this phase. An explanation of the doublet observed in all three spectra in figure 7 might be a Fermi resonance of the 350 cm^{-1} (B_{3g}) vibration with the combination band of the 115 cm^{-1} (B_{3u}) and the 226 cm^{-1} (B_{2u}) vibrations. Because of the symmetry in the crystal, this resonance is possible. We cannot ascertain that the doublets in our α- and γ-phase spectra derive from a Fermi resonance as well, but the Davydov splitting calculated for both phases is much too small to account for the observed separation of the two peaks.

In the 3070 cm^{-1} region, shown in figure 8, we observe in the spectra of all three phases two main lines that are structured. These lines are attributed to the 3065 cm^{-1} (B_{3g}) and the 3070 cm^{-1} (A_g) vibrations. Since the structure is also observed in the β-

phase spectrum, we again think that it might be caused by a Fermi resonance with close-lying overtones or combination bands.

A number of Raman lines are observed between 1050 cm^{-1} and 1110 cm^{-1} as shown in figure 9. The spectra are very similar for all three phases of DCB. We observe two strong lines, one at about 1102 cm^{-1} and one at 1106 cm^{-1}. These two strong lines are also reported in [26], in which the phosphorescence of α- and γ-DCB at low temperatures was studied. The splitting was previously interpreted as a Davydov splitting [26]; this cannot be true because we also observe it in β-DCB. It might be due to a Fermi resonance between the strong 1096 cm^{-1} (A_g) vibration and various overtone or combination bands. The observation of two lines at 1068 cm^{-1} and at 1072 cm^{-1} was also reported [26], assigned to the $0 \rightarrow 2\,550$ cm^{-1} (B_{1u}) vibration, in Fermi resonance with the (A_g) vibration. All other bands in figure 9 may also be caused by Fermi resonances, but the assignment is difficult. Spectra at 77 K, not shown here, exhibit lines which are almost a factor of 2 broader than those at 1.2 K. The most likely explanation is that the increase of linewidths at higher temperatures is caused by a decrease of the vibron lifetime. The same effects are also observed in the Raman spectra of TCB [1].

6. Conclusions

From the lattice dynamics calculations on β- and α-DCB it is clear that these two phases are not quasi one-dimensional, neither with respect to the lattice modes nor with respect to the propagation of the internal vibrations. However, to our surprise the low temperature γ-phase shows a nice one-dimensional behaviour of some internal vibrations, although the phonon frequencies vary in all three directions of the Brillouin zone.

In contrast to TCB, where the calculated dispersion of the internal modes could only match the experimentally observed values when fractional atomic charges were added to the potential, the dispersion in the three phases of DCB is mainly caused by the exponential (exchange) terms and partly compensated by the attractive r^{-6} terms. Addition of charges in DCB hardly influences the results. So it is striking that in all three phases of DCB a mechanism different from that in TCB accounts for the vibron band width.

Not only the one-dimensional vibron band structure, but also the (weak) mixing between vibrons and phonons makes it interesting to study γ-DCB by phosphorescnece and Raman experiments. This vibron–phonon mixing is absent in the other two phases of DCB and, as we saw, also in TCB [1].

Calculation of the Davydov splitting for α- and γ-DCB yields small values ($\leqslant 1$ cm^{-1}), except for some low frequency internal modes. Addition of charges increases these splittings especially in the high frequency region. In the Raman spectra of DCB Davydov splittings are indeed observed for the 298 cm^{-1} (B_{2g}) and for the 1169 cm^{-1} (A_g) vibrations. The observed splittings are in qualitative agreement with the computed values, expecially when charges are included in the potential. Some other modes also show splittings which have previously been assigned as Davydov splittings, but which we find also to be present in the β-phase spectrum. These splittings might be explained by Fermi resonances with close-lying overtones and combination bands.

The isotope splitting in the Raman spectrum of the 328 cm^{-1} (A_g) vibration observed in α- and γ-DCB is in quantitative agreement with our calculation of the internal modes of DCB for different chlorine isotopes. In these two phases the splitting is visible because

the vibron band width appears to be small compared with the isotope shifts (the separated band limit). Because of the much larger vibron band width of the same vibration in β-DCB (calculated to be in the order of 10 cm^{-1}) the β-phase Raman spectrum does not show the separated bands but instead shows a complicated band structure. So there is beautiful agreement between calculation and experiment also in this respect.

Because of the breaking of the selection rules due to isotopic disorder we observe in the Raman spectrum the two *ungerade* vibrations (226 cm^{-1} (B_{2u}) and 550 cm^{-1} (B_{1u})) which the calculations have predicted to be most sensitive to the chlorine mass. Isotope effects for *gerade* vibrations other than the 328 cm^{-1} (A_g) vibration could not be detected, again in agreement with the calculations.

The lines observed in the Raman spectrum of all three DCB phases between 1050 cm^{-1} and 1110 cm^{-1} are difficult to assign, but they are most probably due to Fermi resonances of the strong fundamental (A_g) transition with overtones and combination bands.

Acknowledgments

We thank A M Frens for valuable assistance with the Raman experiments. This investigation is part of the research programme of the 'Stichting voor Fundamenteel Onderzoek der Materie' (FOM) and the 'Stichting Scheikundig Onderzoek in Nederland' (SON), financially supported by the 'Nederlandse Organisatie voor Wetenschappelijk Onderzoek' (NWO).

References

[1] Jongenelis A P J M, van den Berg T H M, Jansen A P J, Schmidt J and van der Avoird A 1988 *J. Chem. Phys.* **89** 4023
[2] Bonadeo H and D'Alessio E A 1973 *Chem. Phys. Lett.* **19** 117
[3] Bonadeo H, D'Alessio E, Halac E and Burgos E 1978 *J. Chem. Phys.* **68** 4714
[4] Reynolds P A, Kjems J K and White J W 1974 *J. Chem. Phys.* **60** 824
[5] Abramson E H, Jongenelis A P J M and Schmidt J 1987 *J. Chem. Phys.* **87** 3719
[6] Housty J and Clastre J 1957 *Acta Crystallogr.* **10** 695
[7] Croatto U, Bezzi S and Bua E 1952 *Acta Crystallogr.* **5** 825
[8] Frasson E, Garbuglio C and Bezzi S 1959 *Acta. Crystallogr.* **12** 126
[9] Gehlfenstein M and Szwarc H 1971 *Mol. Cryst. Liq. Cryst.* **14** 283
[10] Wheeler G L and Colson S D 1975 *Acta Crystallogr.* B **31** 911
[11] Wheeler G L and Colson S D 1976 *J. Chem. Phys.* **65** 1227
[12] von Borczyskowski C and Kirski T 1987 *J. Lumin.* **38** 295
[13] Grimm J and von Borczyskowski C 1988 *J. Lumin.* **40–1** 645
[14] Reynolds P A, Kjems J K and White J W 1972 *J. Chem. Phys.* **56** 2928
[15] Burgos E, Bonadeo H and D'Alessio E 1975 *J. Chem. Phys.* **63** 38
[16] Taddei G, Bonadeo H, Marzocchi M P and Califano S 1973 *J. Chem. Phys.* **58** 966
[17] Califano S, Schettino V and Neto N 1981 *Lattice dynamics of molecular crystals* (Berlin: Springer)
[18] Neto N, Taddei G, Califano S and Walmsley S H 1976 *Mol. Phys.* **31** 457
[19] Neto N and Kirin D 1979 *Chem. Phys.* **44** 245
[20] Scherer J R 1964 *Spectrochim. Acta* **20** 345
[21] Scherer J R 1967 *Spectrochim. Acta* A **23** 1489
[22] Wilson E B, Decius J C and Cross P C *Molecular vibrations* (New York: McGraw-Hill)
[23] van Kooten J F C and Schmidt J 1985 *Chem. Phys. Lett.* **117** 77
[24] Janes S M and Brenner H C 1986 *Chem. Phys.* **101** 429
[25] Bellows J C, Prasad P N, Monberg E M and Kopelman R 1978 *Chem. Phys. Lett.* **54** 439
[26] Gash B W, Hellmann D B and Colson S D 1972 *Chem. Phys.* **1** 191